PNAS RESEARCH ARTICLE | MEDICAL SCIENCES

17β-estradiol promotes extracellular vesicle release and selective miRNA loading in ERα-positive breast cancer

Rares Drula[a,b,1], Barbara Pardini[c,d,1,2], Xiao Fu[e,f,1], Mireia Cruz De los Santos[e,g,1], Ancuta Jurj[a,b,1], Lan Pang[a,1], Sherien M. El-Daly[e,h], Linda Fabris[a], Erik Knutsen[e,i,j], Mihnea P. Dragomir[e,k,l,m], Recep Bayraktar[a], Yongfeng Li[e,n], Meng Chen[a], Filippo Del Vecchio[o], Léa Berland[e,p], Jessica Dae[e,q], Daniel Fan[a,q], Masayoshi Shimizu[a], Anh M. Tran[e,r], Mercedes Barzi[s], Carlotta Pioppini[e,t], Angelica M. Gutierrez[u], Cristina Ivan[e,v,3], Salyna Meas[w], Carolyn S. Hall[w,4], Suresh K. Alahari[x], Ioana Berindan-Neagoe[b], Muller Fabbri[o,y], Anthony Lucci[w], Banu Arun[u], Simone Anfossi[a], and George A. Calin[a,v,2]

Edited by Myles Brown, Dana-Farber Cancer Institute, Boston, MA; received December 6, 2021; accepted April 14, 2023

The causes and consequences of abnormal biogenesis of extracellular vesicles (EVs) are not yet well understood in malignancies, including in breast cancers (BCs). Given the hormonal signaling dependence of estrogen receptor–positive (ER+) BC, we hypothesized that 17β-estradiol (estrogen) might influence EV production and microRNA (miRNA) loading. We report that physiological doses of 17β-estradiol promote EV secretion specifically from ER+ BC cells via inhibition of miR-149-5p, hindering its regulatory activity on SP1, a transcription factor that regulates the EV biogenesis factor nSMase2. Additionally, miR-149-5p downregulation promotes hnRNPA1 expression, responsible for the loading of let-7's miRNAs into EVs. In multiple patient cohorts, we observed increased levels of let-7a-5p and let-7d-5p in EVs derived from the blood of premenopausal ER+ BC patients, and elevated EV levels in patients with high BMI, both conditions associated with higher levels of 17β-estradiol. In brief, we identified a unique estrogen-driven mechanism by which ER+ BC cells eliminate tumor suppressor miRNAs in EVs, with effects on modulating tumor-associated macrophages in the microenvironment.

estrogen receptor | extracellular vesicles | exosomes | breast cancer | microRNAs

Cell-to-cell communication through extracellular vesicles (EVs) is a hallmark of life (1). EVs are small membrane–enclosed particles released by virtually all cell types that can mediate both paracrine and endocrine cellular communication (2) via transfer of their molecular cargo to recipient cells (3, 4). Based on their size and biogenesis, EVs can be broadly categorized into exosomes, microvesicles, and apoptotic bodies (5). While their composition is reflective, to some degree, to their cell of origin, their loading, biogenesis, and secretion are highly regulated and can be influenced by physiological conditions (6–9). Alas, little to nothing is known about the role of hormones in the regulation of biogenesis, loading, and secretion of EVs. Recent evidence shows that the obesity-associated adipokine leptin regulates EV secretion in both estrogen receptor–positive (ER+) MCF-7 cells and triple-negative MDA-MB-231 cells (10).

Recently, microRNAs (miRNAs) have been highlighted as mediators of hormone-like intercellular communication (11–14). Tumor-derived EVs containing miRNAs can directly amend tumor cell invasiveness and motility by modulating the TME (15). Although some evidence suggests that the repertoire of miRNAs sorted into EVs differs from the cytoplasmic content of the cell of origin (16, 17), the exact mechanisms of miRNA loading into EVs remain unknown. Several RNA-binding proteins (RBP) have recently been highlighted, such as the members of the heterogeneous nuclear ribonucleoprotein (hnRNP) family, specifically hnRNPA2B1, which can bind certain miRNAs based on the presence of a sequence motif (exomotif) and dictate their loading into exosomes/EVs (18).

Breast cancer (BC) is the most common female malignancy accounting for 30% of all newly diagnosed cancers in women (19), with the ER+ subtype accounting for about 66% of total BC cases (20). As estrogen is one of the main drivers of ER+ tumor growth (21), the standard therapy is the inhibition of estrogen receptor signaling. Despite the initial responsiveness, a large proportion of patients acquires treatment resistance to estrogen inhibitors, causing disease progression (22–24). Metastatic disease is incurable, and the available therapies are palliative (25). Therefore, it is essential to acquire deeper knowledge of the molecular mechanisms of estrogen dependence in BC to reveal therapeutic targets.

Alterations in hormonal signaling have been previously linked to the regulation of miRNA expression (26–29). In several cases, ER activation has been proven to regulate a subset of miRNAs involved in its negative regulation in a tumor-suppressive manner (30).

Significance

The effects of hormones on EV production and loading are still unknown. We describe a mechanism linking estrogen and EVs in BC: 17β-estradiol increases EV production in ER+ BC cells in a dose-dependent manner and enriches specific miRNAs in their cargo, influencing macrophage activation. These effects were also identified in EVs derived from the blood of ER+ BC patients stratified on menopausal status and body mass index. Such findings can be used for biomarker development for BC risk stratification.
We propose a unique mechanism in which estrogen promotes the tumor-suppressing miRNA export from ER+ BC cells, with possible implications in the tumor microenvironment. Such findings can be further exploited therapeutically to improve the ER+ BC patient's survival.

Competing interest statement: G.A.C. is the scientific founder of Ithax Pharmaceuticals.

This article is a PNAS Direct Submission.

[1]R.D., B.P., X.F., M.C.D.I.S., A.J., and L.P. contributed equally to this work.

[2]To whom correspondence may be addressed. Email: barbara.pardini@iigm.it or gcalin@mdanderson.org.

[3]Present address: Caris Life Sciences, 750 W John Carpenter Fwy, Suite 800, Irving, TX 75039.

[4]Present address: Exact Science, 5505 Endeavor Lane, Madison, WI 53719.

This article contains supporting information online at https://www.pnas.org/lookup/suppl/doi:10.1073/pnas.2122053120/-/DCSupplemental.

Published May 30, 2023.

Relevant examples are the let-7 family members, up-regulated following ER activation, hindering the expression of oncogenes such as Ras and c-Myc (31). Conversely, ER expression is also posttranscriptionally regulated by miRNAs, such as the miR-191/425 family (27, 30).

In the present work, we hypothesized that 17β-estradiol signaling could regulate both EV biogenesis and miRNA loading via the downregulation of specific miRNAs posttranscriptionally regulating key factors involved in these processes. We report that ER+ BC cells display increased EV secretion and a selective enrichment into them of let-7 family members in presence of 17β-estradiol and in a dose-dependent manner, including at physiologically relevant levels. The proposed mechanism is dependent on the 17β-estradiol-induced downregulation of miR-149-5p at the cellular level which targets both SP1, a transcription factor for the EV secretion regulator nSMase2 (neutral sphingomyelinase 2), and hnRNPA1, an hnRNP regulating miRNA loading into EVs.

Results

Estrogen Increases the Number of EVs Specifically in ER+ Breast Cancer Cells. The study workflow and experimental design are presented in Fig. 1*A*. To test whether 17β-estradiol can regulate the secretion of EVs, we first selected three ER+ cell lines, MCF-7 (ER+, PR+, HER2–), BT-474 (ER+, PR+, HER2+), and ZR-75-1 (ER+, PR–, HER2–), as well as the triple-negative BC (TNBC) cell line MDA-MB-231 (ER–, PR–, HER2–) and MCF-10A, an immortalized ER– human breast epithelial cell line, as negative controls (*SI Appendix*, Fig. S1*A*). The cells were treated with 10 pM, 100 pM, 1 nM, or 10 nM of 17β-estradiol (Fig. 1*B*). The first two doses are the closest to the physiologic levels of estrogen in women (32, 33), whereas the latter are the most commonly used in vitro (34, 35). Stimulation with 17β-estradiol significantly increased the amount of EVs with exosome-like size (about 75 to 200 nm) in the supernatants of ER+ cells compared to their unstimulated controls (Fig. 1*B* and *SI Appendix*, Fig. S1*B*), with no morphological modifications (*SI Appendix*, Fig. S1*C*) being observed following treatment. The amplitude of the EV enrichment was proportional to both 17β-estradiol dose and expression levels of ER by each cell line (excepting ZR-75-1 with 10pM 17β-estradiol, Fig. 1*B*). The highest levels of EV enrichment were noticed in the case of MCF-7 and BT-474, and marginally in ZR-75-1, the ER+ cell line with the lowest expression of ER (*SI Appendix*, Fig. S1*A*). We also observed an ER+-like trend for MCF-10A that expresses very low levels of ER. Although significant, the production of EVs in MCF-10A was discrete in comparison to the production seen in ER+ cell lines after 17β-estradiol treatment. We tested whether this response to treatment was due to the expression of an alternative 17β-estradiol receptor, the G-protein-coupled estrogen receptor 1 (GPER1 or GPR30) (36, 37) (*SI Appendix*, Fig. S1*A*). We assessed the EV levels in MCF-10A (which has the highest levels of GPER1) treated with 17β-estradiol in presence of a GPER1-selective agonist [G1, 100 nM (38)] or antagonist [G36, 500 nM (39)]. We did not observe significant changes in EV levels (*SI Appendix*, Fig. S1*D*), allowing us to potentially exclude the involvement of GPER1 in the EV release mechanism in MCF-10A cells. This, along with the observed higher sensitivity of the ER+ cells to 17β-estradiol, indicates that GPER1 might play a secondary role in estradiol effects and that the observed response in MCF-10A could be due to residual ER-α activity.

To confirm whether the EV production mechanism is dependent on the ER pathway activation, we utilized 4-hydroxytamoxifen (4-OHT, 100 nM), a known ER antagonist and ER pathway inhibitor (40, 41) (Fig. 1*C*). We used *GREB1,* a downstream ER-regulated gene indicator (42), to confirm the inhibitory effects of 4-OHT (Fig. 1*D*). Treatment with different combinations of 17β-estradiol (100 pM, 1 nM, and 10 nM) and 4-OHT (10 nM, 100 nM, and 1 μM) confirmed the inhibitory effect of 4-OHT (*SI Appendix*, Fig. S1*E*). EVs in the supernatants of MDA-MB-231 did not increase after 17β-estradiol, while we observed a slight increase in the case of MCF-10A, especially at a high dose of 17β-estradiol (Fig. 1 *B* and *C* and *SI Appendix*, Fig. S1*B*). We found that the 4-OHT treatment alone and in combination with 17β-estradiol was efficient in inhibiting ER pathway activation (Fig. 1*C*), resulting in the ablation of the presumed ER-dependent EV enrichment mechanism in the case of MCF-7 and BT-474, with partial efficiency in the latter given the documented resistance to tamoxifen mediated by the very high HER2 levels (43). The treatments induced no significant effect in the case of MDA-MB-231 cells, yet, in the case of MCF-10A, a slight EV enrichment was observed following the treatment with 4-OHT, followed by a noticeable decrease when in combination with 17β-estradiol (Fig. 1*C*).

To specifically confirm the involvement of the ER pathway in the regulation of EV secretion, we utilized fulvestrant (10 nM), a selective estrogen receptor degrader (SERD) (44) along with 17β-estradiol (1 nM) and in combination (Fig. 1*E*). We observed a strong decrease in EVs following the addition of fulvestrant in the case of MCF-7 and BT-474, partially rescued following the addition of 17β-estradiol (Fig. 1 *E* and *F*). BT-474 displayed a substantial decrease both in the fulvestrant and combination treatments, presumably due to its lower ER-α expression level. No major trends were noticed in ZR-75-1, consistent with the limited response to the previous treatments. On the contrary, the TNBC cell line MDA-MB-231 and the MCF-10A cells displayed no significant response, showing a slight EV decrease in all conditions (Fig. 1*E*). As for the 4-OHT treatments, we confirmed the inhibitory activity of fulvestrant on the activation of the ER pathway by *GREB1* (Fig. 1*F*). Overall, fulvestrant was efficient in determining a decrease in EV production in the main ER+ cell lines, furtherly confirming that the mechanism is at least partially involved in either the EV biogenesis or EV release mechanism.

To further confirm the role of the ER pathway in the regulation of EV secretion, we knocked down ER-α [the main mammary gland ER receptor (45)] with siRNAs in MCF-7, the ER+ cells with the higher expression of ER-α (*SI Appendix*, Fig. S1*F*). This caused a significant decrease in the EV release following 17β-estradiol treatment when compared to the scramble control stimulated with 17β-estradiol (Fig. 1*G*). This indicated that the pattern in the modification of EV production in ER+ cells is influenced by the activation of the estrogen signaling pathway.

To understand the possible factors involved in the induction of EV production mediated by 17β-estradiol, we utilized a documented EV inhibitor, GW4869 (46), a competitive inhibitor of nSMase2, and a key enzyme in EV biogenesis and secretion (47). GW4869 treatment decreased the basal EV secretion in the supernatants of all cells, except for MCF-10A (*SI Appendix*, Fig. S1*G*). Interestingly, the stimulatory effect of 17β-estradiol was partially counteracted by GW4869, indicating that 17β-estradiol is possibly promoting EV secretion via an nSMase2-dependent mechanism. Interestingly, we observed an overall decreasing trend in EV numbers in MCF-7 and MDA-MB-231 that was proportional with the siRNA knockdown of the EV secretion regulator nSMase2 (*SI Appendix*, Fig. S1*H*) in presence of 17β-estradiol, indicating that nSMase2 is involved at least at some degree in regulating EV production.

Estrogen Increases the let-7 Family Abundance in EVs Derived from ER+ Breast Cancer Cells. The observed modifications in the quantity of secreted vesicles might be indicative of the underlying

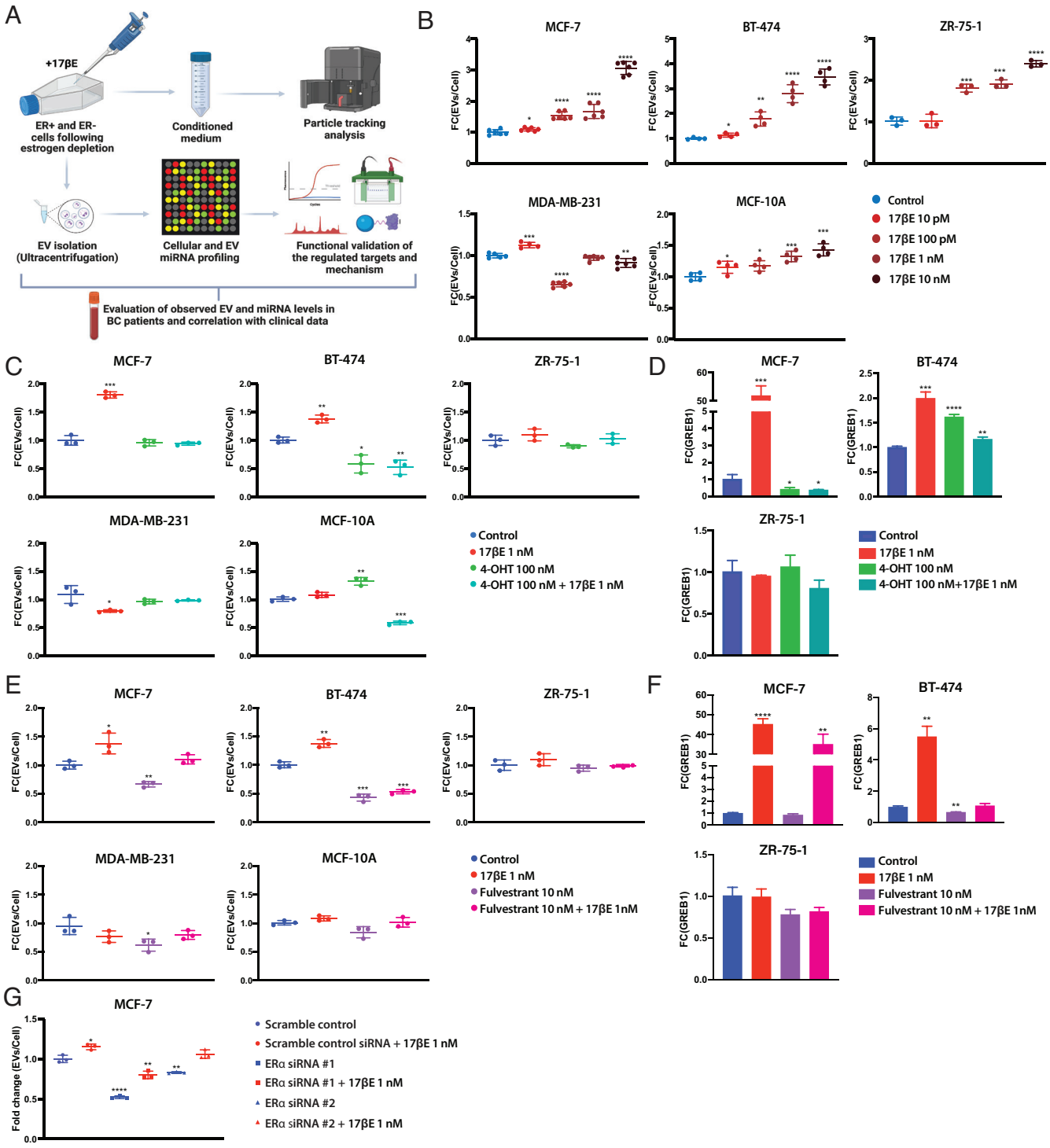

Fig. 1. (*A*) Experimental workflow of the study; (*B*) The relative concentration of secreted particles from MCF-7 (ER+, PR+, HER2−), BT-474 (ER+, PR+, HER2+), ZR-75-1 (ER+, PR-, HER2−), MDA-MB-231 (ER−, PR−, HER2−), and MCF-10A (normal human mammary epithelial cells) obtained from NanoSight not treated and after treatment with 17β-estradiol at different concentrations (10 pM, 100 pM, 1 nM, and 10 nM); (*C*) The relative concentration of secreted particles from MCF-7, BT-474, ZR-75-1, MDA-MB-231, and MCF-10A obtained from NanoSight not treated and after treatment with 17β-estradiol (1 nM), 4-hydroxytamoxifen (4OHT; 100 nM), or both as normalized to the number of cells collected in each experiment; (*D*) Expression levels of cellular *GREB1* as a marker of 17β-estradiol stimulation in MCF-7, BT-474, and ZR-75-1 cells following the treatment with 17β-estradiol (1 nM), 4-hydroxytamoxifen (4OHT, 100nM), or a combination of the two (MDA-MB-231 and MCF-10A were not tested because ER−); (*E*) The relative concentration of secreted particles obtained from NanoSight of MCF-7, BT-474, ZR-75-1, MDA-MB-231, and MCF-10A cell lines not treated and after treatment with 17β-estradiol (1 nM), fulvestrant (10 nM), or both, normalized to the number of cells collected in each experiment; (*F*) Expression levels of cellular *GREB1* as a marker of 17β-estradiol stimulation in MCF-7, BT-474, and ZR-75-1 cells following the treatment with 17β-estradiol (1 nM), fulvestrant (10 nM), or both (MDA-MB-231 and MCF-10A were not tested because ER−); (*G*) The relative concentration of secreted particles obtained from NanoSight of MCF-7 and MDA-MB-231 cell lines after transfection with ER siRNAs and scramble control in the presence of 1 nM 17β-estradiol; FC = fold-change; ERα = estrogen receptor; 17βE = 17β-estradiol; 4-OHT = 4-hydroxytamoxifen. *P = 0.05; **P = 0.01; ***P = 0.001; ****P = 0.0001.

effects dictated by their cargo composition, which may include posttranscriptional regulators such as miRNAs and long noncoding RNAs (18, 48). Therefore, we performed a genome-wide miRNA microarray analysis on the RNA extracted from MCF-7 cells (selected due to its potent estrogen signaling activation; *SI Appendix*, Fig. S1*A*) and MDA-MB-231 cells (as control) and their derived EVs from both

unstimulated and 17β-estradiol-stimulated conditions (Fig. 2*A* and GEO series accession number GSE127787).

The global miRNA profiles greatly differed between the cell lines and their corresponding secreted EVs (Fig. 2 *A* and *B* and *SI Appendix*, Table S1). This difference was particularly noticeable between 17β-estradiol-stimulated MCF-7 cells and EVs when compared to nontreated counterparts (Fig. 2*B*). In MCF-7, we noticed a significant downregulation of cellular miR-149-5p following 17β-estradiol treatment, whereas most miRNAs of the let-7's family were up-regulated at EV and cellular levels (Fig. 2*B* and *SI Appendix*, Fig. S2*A*). No significant changes in these miRNAs were found in MDA-MB-231-derived EVs between conditions. Among all the significantly up- or down-regulated miRNAs after 17β-estradiol treatment, none were in common between MCF-7 and MDA-MB-231 cells or EVs (Fig. 2*C*). We next validated by qRT-PCR the expression of let-7a-5p and let-7d-5p in paired EVs and all cell lines before and after 17β-estradiol treatment (10 nM) and noticed similar patterns consistent with the microarray results (Fig. 2*D*). The upregulation of the let-7 members at the cellular level was significant especially in MCF-7 and to a lesser extent in ZR-75-1, but not in BT-474 cells (Fig. 2*D*). Interestingly, similar results by qRT-PCR were obtained also for 17β-estradiol treatment at lower concentration (1 nM) closer to the physiological levels in the blood of premenopausal women (*SI Appendix*, Fig. S2*B* for cellular levels and *SI Appendix*, Fig. S2*C* for EV levels). All the ER+ cell lines showed a significant EV enrichment in either one of let-7a-5p, let-7c-5p, and let-7d-5p after 17β-estradiol treatment not visible in the ER-negative cells (*SI Appendix*, Fig. S2 *B* and *C*). These results indicate that ER signaling, besides promoting EV secretion, is also involved in modulating the abundance of specific miRNAs in EVs, and this effect is proportional to the estrogen dose at least for the let-7 family of miRNAs.

Estrogen Specifically Down-Regulates miR-149 in ER+ Cells by Binding to ER-Binding Motif Promoter Regions. We followed with the exploration of the role of estrogen in miR-149-5p downregulation in ER+ cells. First, we validated by qRT-PCR the downregulation of miR-149-5p observed in the microarray (Fig. 3*A*) and noticed a dose-dependent downregulation of miR-149-5p in MCF-7 following treatment with three 17β-estradiol doses (100 pM, 1 nM, and 10 nM; Fig. 3*A*), not observable in MDA-MB-231. Moreover, an upregulation of miR-149-5p following the abrogation of the ER pathway using 4-OHT was indicative of the regulatory activity of the ER pathway upon miR-149-5p (Fig. 3*B*). The effect was partly rescued following the addition of 17β-estradiol, effects that were not noticeable in MDA-MB-231 (Fig. 3*B*). This cumulating evidence further indicates that the regulation of miR-149-5p is dependent on the functionality of the estrogen signaling pathway.

To the current date, little is known about the regulatory effect of hormones on miRNAs, as transcript start sites (TSS) and promoter regions of pri-miRNA transcripts are poorly characterized (50, 51) given the difficulty in the characterization of miRNA promoters and enhancers associated with transcription factor (52).

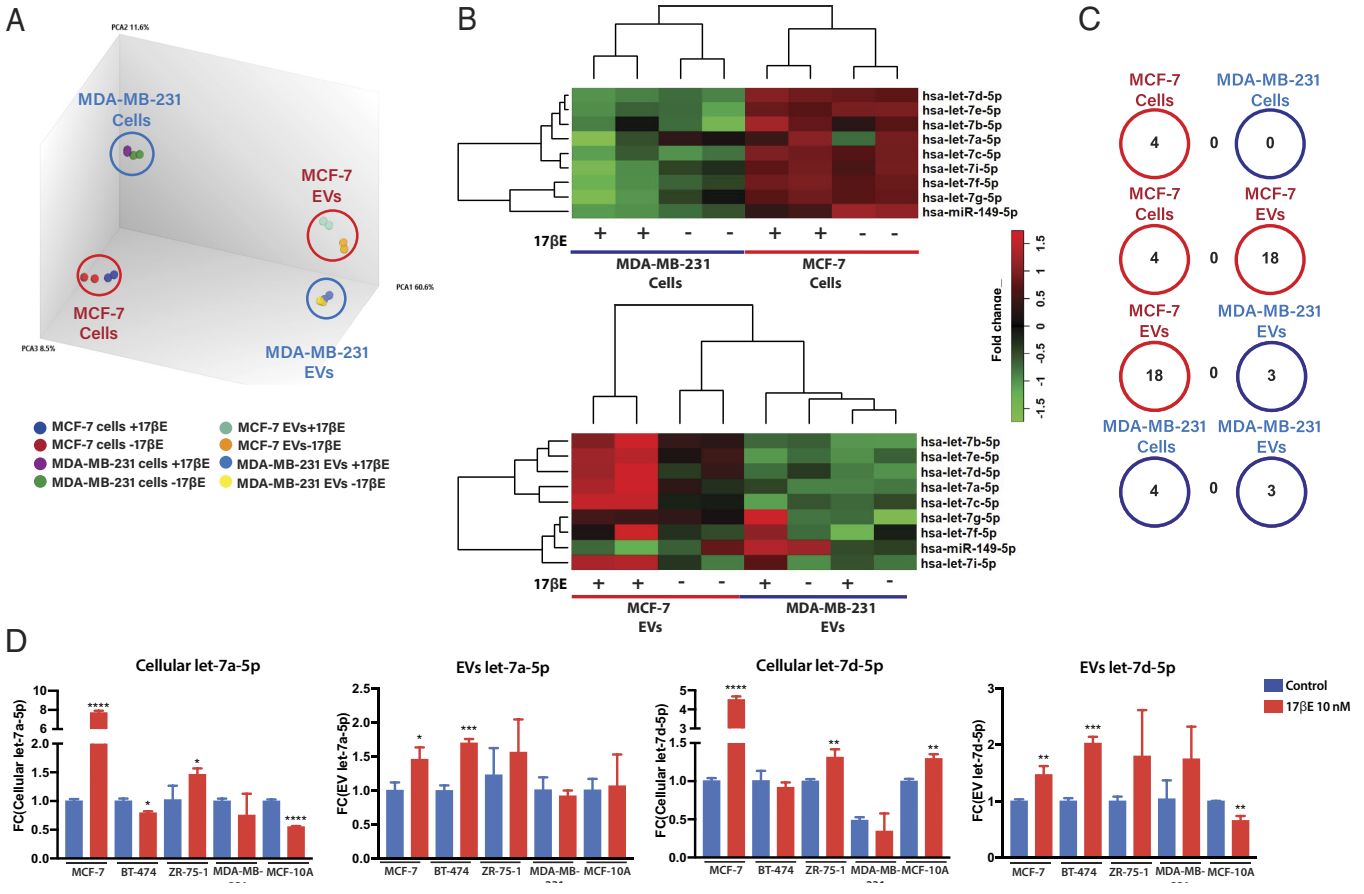

Fig. 2. (*A*) Principal component analysis (PCA) loading displaying the clustering of the investigated sample sets used for the Affymetrix GeneChip miRNA Array 3.0; (*B*) Heat maps from the microarray analysis of cellular (*Upper*) and EV (*Lower*) miRNAs from MCF-7 and MDA-MB-231 with or without 17β-estradiol treatment (10 nM) highlighting the main up- or down-regulated miRNAs; (*C*) Venn diagrams based on the miRNA microarray data indicating the nonoverlapping differential miRNA signatures in cell and EVs between MCF-7 (red) and MDA-MB-231 (blue); (*D*) Validation by qRT-PCR of the expression levels of let-7a-5p (*Left*) and let-7d-5p (*Right*) in EVs and cells lines (MCF-7, BT-474, ZR-75-1, MDA-MB-231, and MCF-10A) with or without 17β-estradiol treatment (10 nM). 17βE = 17β-estradiol ; FC = fold-change. **P* = 0.05; ***P* = 0.01; ****P* = 0.001; *****P* = 0.0001.

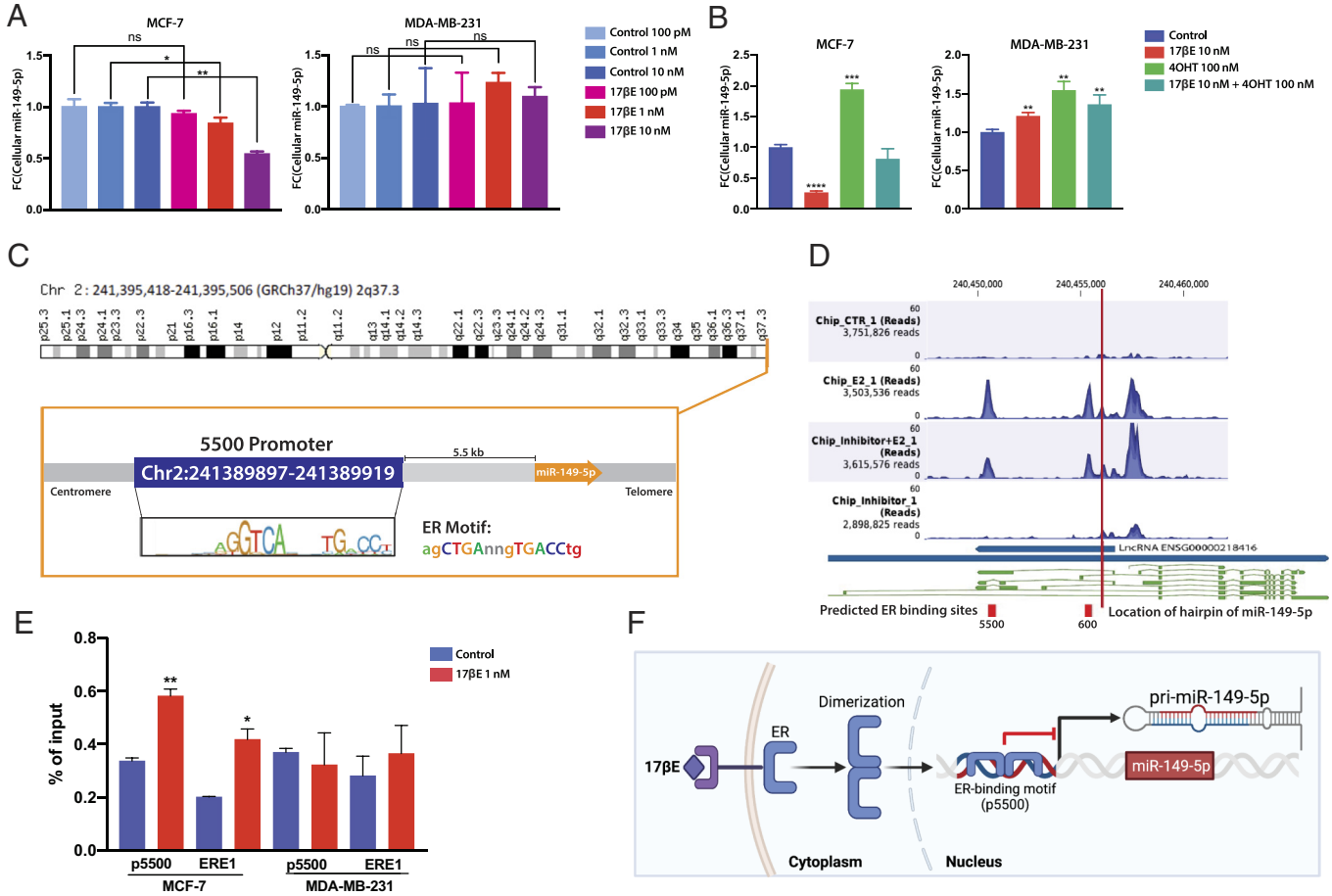

Fig. 3. (*A*) Expression levels of cellular miR-149-5p in MCF-7 and MDA-MB-231 following 100 pM, 1 nM, and 10 nM 17β-estradiol stimulation (three independent experiments); (*B*) Expression level of cellular miR-149-5p in MCF-7 and MDA-MB-231 after treatment with 10 nM 17β-estradiol, 100 nM 4-OHT, and their combination; (*C*) The genomic region of *MIR149* from the UCSC Genomic Browser, GRCh37/hg19 with the 5 kb upstream region ("5500" promoter or p5500) containing the motif for ER1 binding; (*D*) Genomic area of *MIR149* showing the presence of two predicted ER-binding sites (at −5,500 and −600 from the starting point of miR-149) (bottom of the figure). Chip-Seq map generated from the study of Sun et al. (49) indicating the peak in the ER-interacting region overlapping with the "5500" promoter region of miR-149-5p (extended version of the panel in *SI Appendix*, S3*D*); (*E*) Chip-qPCR analysis indicating the enrichment levels of the p5500 and ERE1 regions in MCF-7 and MDA-MB-231 in control and estrogen-stimulated cells following ER immunoprecipitation; (*F*) Diagram describing the regulatory mechanism of 17β-estradiol on miR-149-5p. FC = fold-change; 17βE = 17β-estradiol; 4-OHT = 4-hydroxytamoxifen; **P* < 0.05, ***P* = 0.01; ****P* = 0.001; *****P* = 0.0001; ns = not significant.

On the contrary, an important process following ER activation is its dimerization and nuclear translocation which allows the binding to specific genomic sequences called estrogen receptor elements (EREs) that activate or repress transcription of specific genes (53). As such, we hypothesized that miR-149-5p is transcriptionally repressed by ER-α through direct targeting of its promoter region. To test this, we used sequence-transcription stimulation by an adjacent heterologous promoter region as previously described (54). We identified a region containing the predicted ER-α-binding motifs 5 kb upstream of miR-149, hereby called "5500" (Fig. 3*C*). First, we validated the functionality of the promoter region by subcloning it into a vector containing the luciferase gene (*SI Appendix*, Fig. S3*A*). The cloned insert "5500" resulted in a significant increase in luciferase activity (*SI Appendix*, Fig. S3*B*), which was lost following the deletion of the 16bp ER-α interaction region (*SI Appendix*, Fig. S3*C*), confirming the promoter function of the sequence.

Next, to investigate the potential binding interaction between ER and our region of interest, we utilized an independent publicly available ER Chip-Seq (49) dataset that included MCF-7 cells treated with 10 nM 17β-estradiol and in combination with 50 μM EHT 1864, a Rac inhibitor with proven efficacy in hindering ER promoter–binding ability (55). Three ER Chip-Seq peaks were identified in the ER stimulated set, located −5,500 bp (peak score: 4.05, *P*-value = 0.00003), −600 bp (peak score: 3.24, *P*-value = 0.0006), and +1,500 (peak score: 3.00, *P*-value = 0.001) from the miR-149 hairpin. Following the comparison of the peaks in all conditions, the peak at −5,500 was the only showing consistent reduction following EHT 1864 treatment and no overlapping with the control conditions, indicative of a real ER interaction site (Fig. 3*D* and *SI Appendix*, Fig. S3*C*).

We validated the interaction utilizing ER ChiP-qPCR and evaluated the enrichment levels of the DNA sequence corresponding to the "5500" potential promoter following 17β-estradiol stimulation and subsequent ER immunoprecipitation. We utilized the estrogen response element 1 (ERE1), a previously confirmed ER-binding region (56) as positive control. The resulting DNA was evaluated using qRT-PCR (Fig. 3*E*). In MCF-7, we observed a significant enrichment in ER-bound DNA corresponding to both the investigated 5500 and ERE1 regions following stimulation, indicative of increased binding of the region following the activation of the ER pathway. On the contrary, no considerable differences in enrichment were found in MDA-MB-231 for both investigated regions (Fig. 3*E*).

In conclusion, the consistent downregulation of miR-149-5p in ER+ cells in conjunction with the confirmed enhanced interaction between ER-α and the miR-149-5p 5500 promoter region following 17β-estradiol treatment is strongly indicative of an estrogen-dependent regulation of miR-149-5p (Fig. 3*F*).

miR-149-5p Targets both SP1 and hnRNPA1 and 17β-Estradiol-Mediated Downregulation of miR-149-5p Alters Essential Genes for EV Production and Loading Pathways. To assess the regulatory activity and biological effect of the ER-dependent downregulation of miR-149-5p, we investigated the targets potentially involved in relevant regulatory processes. Using TargetScan (http://www.targetscan.org/vert_72/) and miRwalk 3.0 (http://mirwalk.umm.uni-heidelberg.de/) databases, we identified the transcription factor SP1 and the RNA-binding hnRNPA1 as direct targets of miR-149-5p (Fig. 4*A*). These interactions were also previously confirmed in vitro (57). We tested the interaction and its targets in cell models using anti-miR-149 knockdown in unstimulated MCF-7 and MDA-MB-231 cells and confirmed the upregulation of SP1 and hnRNPA1 by western blot (Fig. 4*B*). Additionally, we validated the SP1 transcription factor activity upon nSMase2 expression by knocking down SP1 using anti-SP1 siRNA transfection (*SI Appendix*, Fig. S4*A*).

The increase of SP1 and hnRNPA1 levels in ER+ and ER- cell lines was confirmed by western blot after treatment with 17β-estradiol (1 nM and 100 pM) as a result of the cellular downregulation of miR-149-5p (Fig. 4*C* and *SI Appendix*, Fig. S4*B*). As expected, MCF-7 exhibited increased levels of SP1 and hnRNPA1 after 17β-estradiol stimulation, which decreased with fulvestrant downregulation of the ER (Fig. 4*C*). The differences were not significant in MDA-MB-231. Interestingly, in MCF-10A, the upregulation of hnRNPA1 was detectable following 17β-estradiol and fulvestrant stimulation (Fig. 4*C*), and no effect on the SP1 target was identified. In brief, miR-149-5p targets and regulates essential genes from EV production and loading pathways.

Members of the let-7 Family Interact with hnRNPA1 When Up-Regulated by 17β-Estradiol Stimulation. Since we observed an increment of EV let-7s following 17β-estradiol stimulation, we investigated the potential mechanism of this specific sorting of cellular miRNAs into EVs. miRNA sorting into EVs is controlled by RNA-binding proteins (RNPs), such as hnRNPA2B1 (18), MVP (58), and SYNCRIP (59). Using RBPmap (http://rbpmap.technion.ac.il/), we found that RBM28, hnRNPA1, hnRNPA2B1, MSI1, MBNL1, DAZAP1, SRSF5, and hnRNPM can bind multiple let-7 family members (Fig. 4*D*). We chose to focus on hnRNPA1 due to being a validated target of miR-149-5p (60) and reported as up-regulated in multiple types of cancer (61, 62), including BC (63).

Recently, it has been found that specific miRNAs can be preferentially loaded into EVs based on the presence of specific short motifs within their sequence (64). These motifs presumably allow the binding of hnRNP family members that mediate their selective

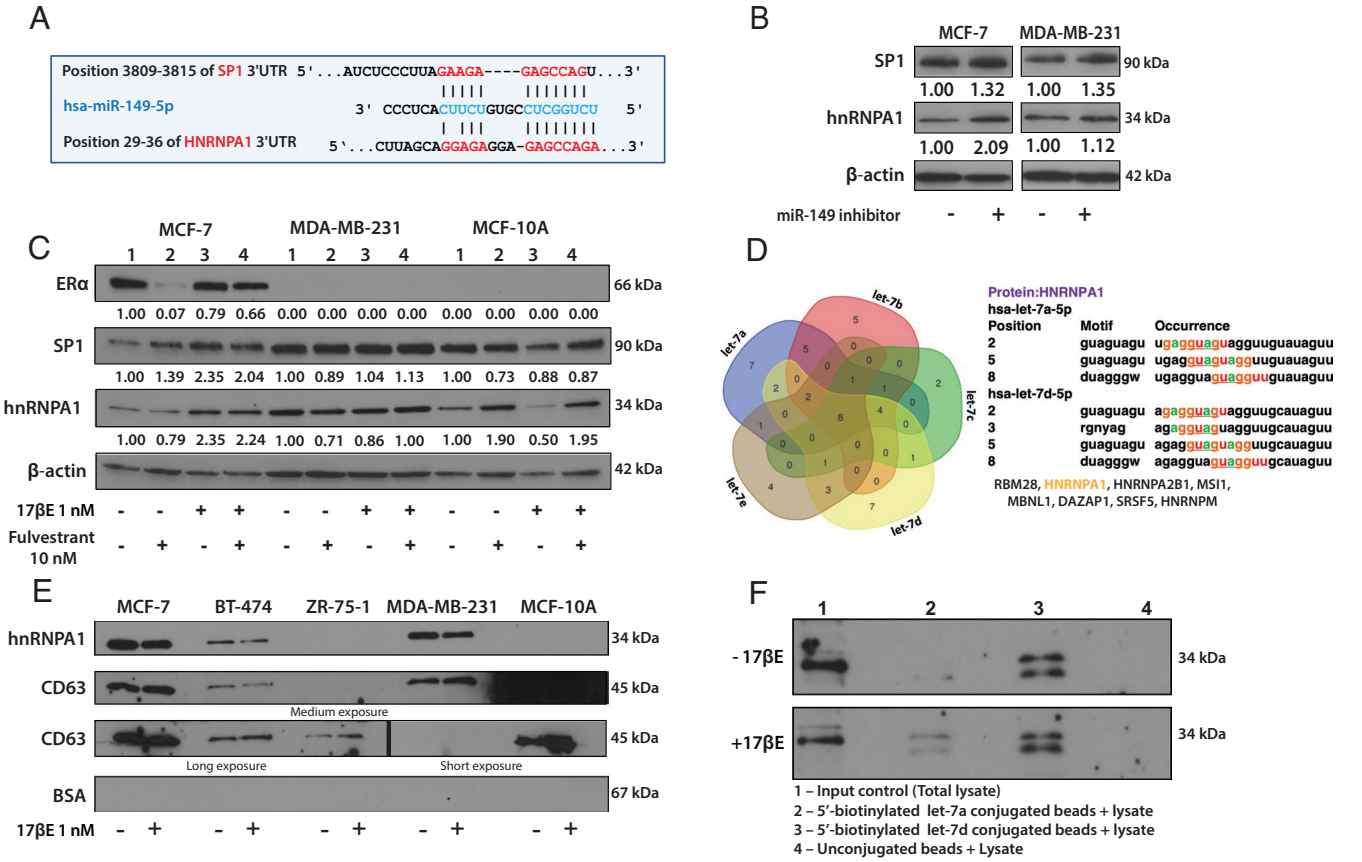

Fig. 4. (*A*) Pairing schemes of complementary miRNA–target interactions between miR-149-5p and 3′UTRs of *SP1* and *HNRNPA1*; (*B*) The expression levels of SP1 and hnRNPA1 measured by western blot analysis following transfection with scrambled RNA and miR-149-5p inhibitor in MCF-7 and MDA-MB-231; (*C*) The expression levels of SP1 and hnRNPA1 measured by western blot analysis in MCF-7, MDA-MB-231, and MCF-10A cells not treated and after treatment with 17β-estradiol (1 nM), fulvestrant (10 nM), or both; (*D*) Venn diagram depicting the predicted RNA-binding proteins interacting with the let-7 family (*Left*) and highlighted EXO motifs for hnRNPA1 binding in the let-7a and let-7d sequences (*Right*) as detected with the RBP map tool; (*E*) Western blot analysis of EV-derived proteins from MCF-7, BT-474, ZR-75-1, MDA-MB-231, and MCF-10A cell lines, highlighting the enrichment of hnRNPA1 in the EVs (for CD63, we showed also a lower and higher exposures of membrane for a full appreciation of the presence of the protein in all cell lines); (*F*) Western blot analysis of hnRNPA1 biotin–streptavidin pull-down assays using biotinylated let-7a-5p and let-7d-5p probes. Input control (lane 1) indicates 20 μg total cell lysate. Lanes 2 and 3 indicate the eluted bound hnRNPA1-let-7a and -let-7d following incubation with 1 mg of total MCF-7 cellular lysate. Lane 4 corresponds to the eluted proteins resulting from the incubation of 1 mg cellular lysate with unconjugated streptavidin beads. 17βE = 17β-estradiol.

sorting into EVs (64–66). Villaroya-Beltri et al. demonstrated that hnRNPA2B1 mediates the selective sorting into EVs of miRNAs that harbor within their sequences the specific GGAG motif (EXO-motif) (18). We hypothesized that hnRNPA1 might work similarly since it has already been demonstrated the presence of a preferential binding site for miR-198 (67). Using the RBP map tool, we identified the presence of the hnRNPA1-specific GGAG EXO-motif binding in EV up-regulated let-7a-5p, -7b-5p, -7c-5p, -7d-5p, and -7e-5p (Fig. 4*D* and *SI Appendix,* Fig. S4*C*).

To deepen the role of hnRNPA1, we first confirmed its enrichment in the EVs derived from all cell lines, excepting MCF-10A (Fig. 4*E*). The purity of the EV protein fraction was confirmed via the detection of CD63, a validated EV marker, and bovine serum albumin (BSA) to exclude protein contamination from the culture media. Additionally, we noticed no major differences in the level of hnRNPA1 in the EVs following 17β-estradiol stimulation, indicating that the hnRNPA1 trafficking does not determine its accumulation in the EVs.

To demonstrate the direct interaction between hnRNPA1 and let-7 family members, we utilized biotin-labeled let-7a-5p and let-7d-5p probes to perform an RNA–protein pull-down. We confirmed the interaction between the biotinylated miRNA probes and hnRNPA1 using both stimulated and unstimulated MCF-7 cells. The interaction was evident in the case of let-7d-5p due to its high enrichment in EVs, but also noticeable (albeit with less intensity) for let-7a-5p, especially following 17β-estradiol stimulation (Fig. 4*F*). The multiple bands are presumably corresponding to posttranslational modifications of hnRNPA1 often observed in the case of hnRNP family members (18). Overall, this proves that let-7 miRNAs harboring the GGAG EXO-motif can directly bind hnRNPA1, regulating their selective loading into EVs.

EV Content of let-7 Family Members in Breast Cancer Patients. We investigated the expression levels of let-7a-5p and let-7d-5p in EVs isolated from two cohorts of BC patients (*SI Appendix,* Table S2). The training set consists of the plasma of 49 BC women, whereas the validation set consists of 96 BC serum samples, grouped according to the subtype (ER+ or TNBC) and compared according to the menopause status (pre- vs. post-menopause). We found significantly higher median levels of let-7a-5p and let-7d-5p in EVs from ER+ premenopausal women compared with those from ER+ postmenopausal women in both cohorts ($P < 0.05$) (*Upper* panels of Fig. 5 *A* and *B*, respectively, for the training and validation sets). No significant differences were observed between pre- and post-menopausal women in the TNBC group for both cohorts (*Lower* panels of Fig. 5 *A* and *B*, respectively, for the training and validation sets). Hence, we can conclude that enrichment in circulating EVs loaded with let-7a-5p and let-7d-5p can be detected in the blood of ER+ pre-menopausal BC women that have on average higher levels of estrogen compared with post-menopausal BC women (68). This enrichment was not found in an additional set of serum samples from 27 women with ER+ BC (pre- or post-menopausal status) receiving adjuvant endocrine therapy as standard treatment after the surgery. This further proves the central role of the malignant cells in the described mechanism.

Recently, it has been found that leptin, a hormone produced and secreted by the adipose tissue, induced the secretion of EVs from ER+ and TNBC cells and its levels correlate with the percentage of body adipose tissue; therefore, we wanted to evaluate whether the amount of EVs in the blood of BC patients correlated with body mass index (BMI) (69). Indeed, we found that the serum of ER+ BC patients with BMI ≥ 25 kg/m^2 (overweight and obese) had higher median levels of EVs than the serum of ER+ BC patients with BMI < 25 kg/m^2 (Fig. 5 *C*, *Upper* panel). We measured a slight increase in EV counts in the serum of TNBC patients with BMI ≥ 25 kg/m^2, but the difference was not significant (Fig. 5 *C*, *Lower* panel). We did not find any correlation between BMI values and let-7 miRNAs (let-7a-5p and let-7d-5p). This may be because leptin induces the secretion of EVs but does not play a substantial role in the regulation of the sorting of let-7 miRNAs into EVs. Therefore, because both 17β-estradiol and leptin can induce the secretion of EVs, only a fraction of the total EVs measured in the blood may be enriched in let-7 miRNAs due to ER-mediated regulation.

EVs Derived from 17β-Estradiol-Stimulated BC Cells Can Regulate Macrophage Activation. We investigated whether there are any functional consequences of the increased production of EVs enriched in let-7 family members after 17β-estradiol stimulation. In recent years, there have been multiple studies highlighting the involvement of let-7s in macrophage-specific processes, such as activation (70), polarization (71), and modulation of proinflammatory phenotypes (72). As such, we investigated whether let-7's enriched EVs can influence the macrophages in the TME. For this, we utilized the THP-1 monocyte cell line which we differentiated into M0 macrophages using phorbol 12-myristate-13-acetate (PMA). EVs were isolated from: a) untreated MCF-7, b) 17β-estradiol-treated MCF-7 cells, and c) from 17β-estradiol-stimulated MCF-7 cells in which let-7a-5p, let-7c-5p, and let-7d-5p were knocked down (Fig. 6*A*). The aim was to assess whether the encapsulated let-7s are responsible for any modification at the cytokine level observed in recipient THP-1 cells (Fig. 6*A*). First, we confirmed that the downregulation of the three let-7 family members at the cellular level following anti-let-7 transfection was also reflected at the EV level (anti-let-7-treated EVs), using a scrambled control RNA (scRNA EVs) as control, which did not affect let-7 levels in EVs (*SI Appendix,* Fig. S5*A*). We then confirmed the significant increase of the three let-7s in THP-1 cells treated with the scRNA-transfected EVs, confirming the uptake of EVs by the cells, while the levels in cells treated with the anti-let-7 EVs were similar to the basal levels of the untreated THP-1 cells. These observations were valid for EVs generated from MCF-7 stimulated either with 17β-estradiol at 1nM (Fig. 6*B*) or 10 nM (*SI Appendix,* Fig. S5*B*). Additionally, as indicated by the dose-dependent modification of let-7s loaded in the EVs derived from cells treated with 10 nM 17β-estradiol when compared to 1 nM (Fig. 2*D* and *SI Appendix,* Fig. S2*B*, respectively), we also observed a more significant enrichment of the let-7 family members following treatment of THP-1 cells with EVs derived from 10nM 17β-estradiol-treated MCF-7 (*SI Appendix*, Fig. S5*B*). Following this, we investigated by qRT-PCR a list of let-7 regulatory targets previously described in macrophages. After treatment of EVs derived from 1nM 17β-estradiol-treated MCF-7, we observed that in the case of the scRNA EVs (enriched in let-7 members), there was a significant downregulation in THP-1 cells of the TET2 DNA dioxygenase, a target of the let-7a/d/f cluster in macrophages, involved in facilitating proinflammatory cytokines (Fig. 6*C*) (72). Additionally, following let-7-enriched EV treatment, we observed a significant decrease of interferon-γ (IFN-γ), possibly as a consequence of *TET2* downregulation, as it was previously shown that TET2 mediates the IFN-γ/JAK/STAT signaling pathway to control chemokine expression in monocytic macrophage-like cells (Fig. 6*C*) (73). We also observed a significant downregulation in IL-12A, one of the main regulatory targets of IFN-γ, indicative of an inhibition of the positive feedback loop between these two genes (Fig. 6*C* and *SI Appendix,* Fig. S5*C*) (74). Additionally, IFN-γ is one of the main cytokines linked with the canonical M1

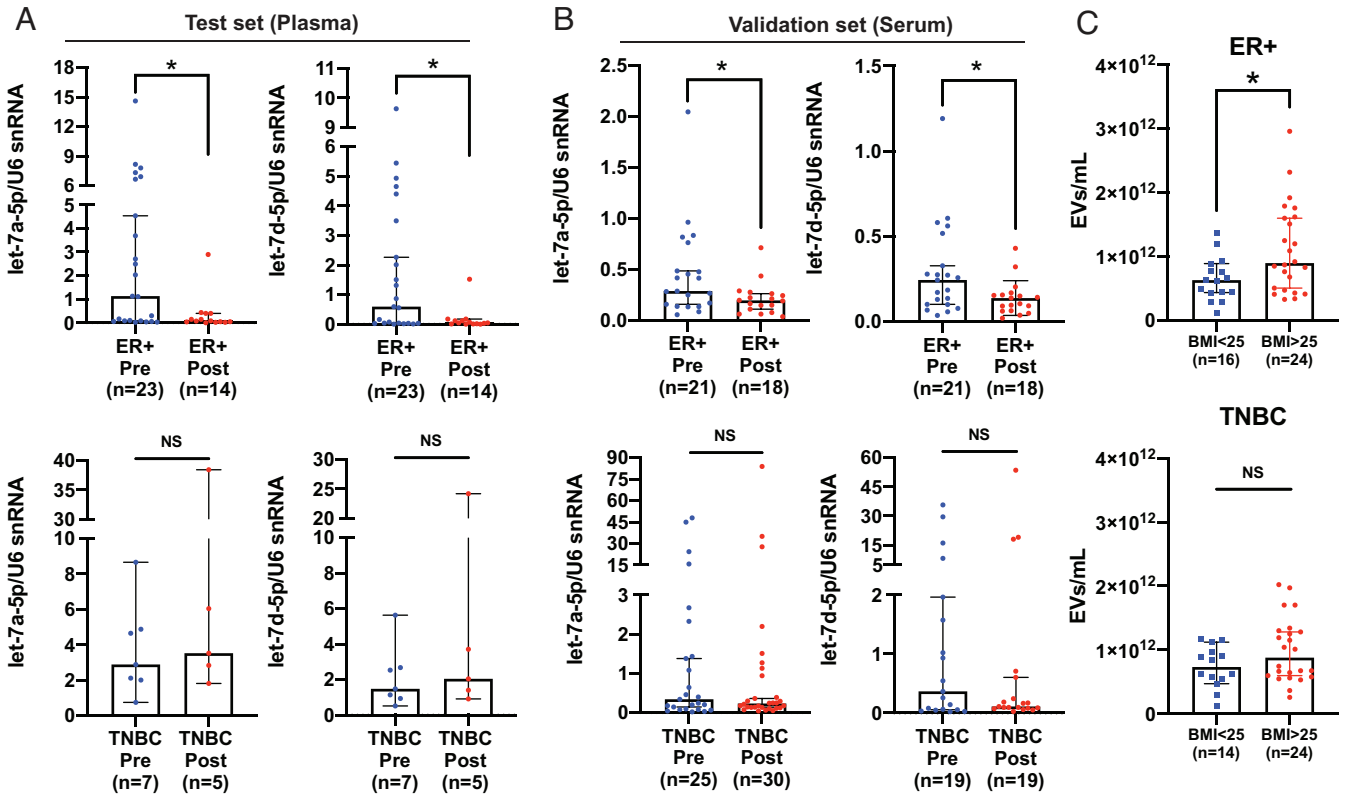

Fig. 5. (*A*) Expression levels of let-7a-5p and let-7d-5p in plasma EVs (test set) from BC women stratified according to the estrogen receptor (ER) and pre/post-menopausal statuses; (*B*) Expression levels of let-7a-5p and let-7d-5p in serum EVs (validation set) from BC women stratified according to the ER and pre/post-menopausal statuses; (*C*) EV amount in the serum of ER+ BC (*Upper*) or TNBC patients (*Lower*) stratified according to BMI [BMI < 25 kg/m^2 (normal weight) or BMI ≥ 25 kg/m^2 (overweight and obese)]. Data are shown as median with 95% CI, Mann–Whitney *U* test was used to compare the medians of the two groups. miR-149-5p was also measured but was not detectable in EVs (we considered it as negative control). ns = non-significant; *P < 0.05.

phenotype activation that is associated with tumor-suppressive properties (75). Other regulatory targets negatively regulated by TET2 included IL-1β which was up-regulated following EV treatment derived from 10nM 17β-estradiol stimulation. Similar results were obtained following the treatments of THP-1 cells with EVs derived from MCF-7 stimulated with 10 nM 17β-estradiol derived from similar conditions (*SI Appendix*, Fig. S5*C*), indicative of the consistency of the effects. In conclusion, EVs derived from 17β-estradiol-stimulated BC cells could modulate the TME by regulating macrophage activation *via* their modified miRNA cargo.

Discussion

In the present work, we reported that EV production in ER+ BC cell lines is modulated by 17β-estradiol in a dose-dependent manner. The response of ER+ cells to this hormone consists of 1) an

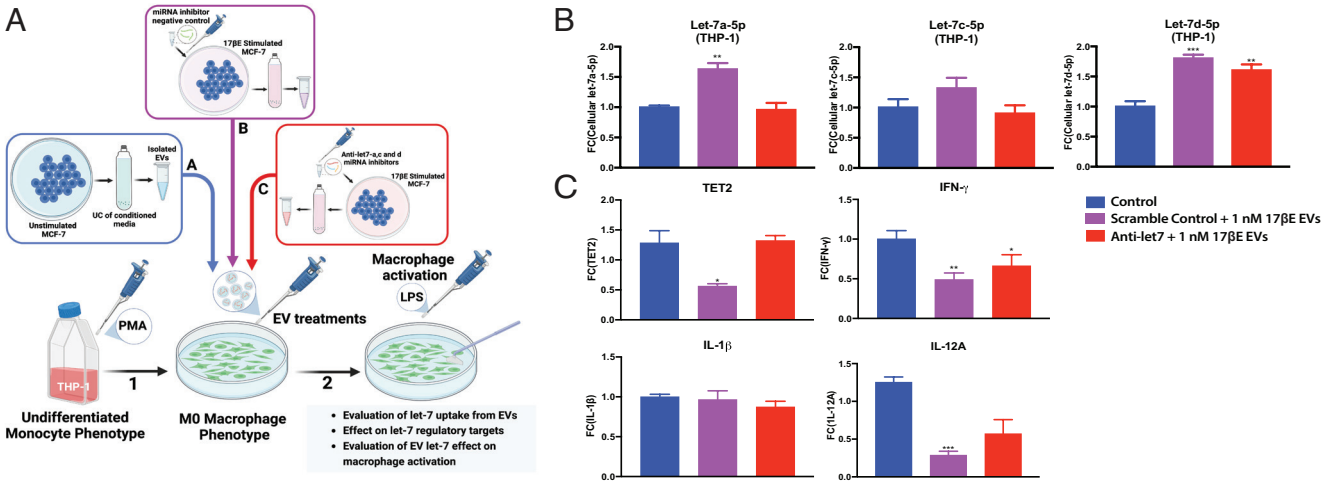

Fig. 6. (*A*) Workflow and experimental design of the EVs and macrophage co-culture experiment; (*B*) Expression levels of let-7a-5p, let-7c-5p, and let-7d-5p in THP-1 cells transfected with EVs derived from untreated MCF-7 (control), 1 nM 17β-estradiol-stimulated MCF-7 cell lines treated with scramble control RNA or with anti-let-7 probes; (*C*) Expression levels measured by qRT-PCR in THP-1 cells of selected cytokines as potential let-7 family regulatory targets after transfection with EVs derived from untreated MCF-7 (control), 1nM 17β-estradiol-stimulated MCF-7 cell lines treated with scramble RNA or with anti-let-7 probes; PMA = phorbol 12-myristate-13-acetate; FC = fold-change. *P = 0.05; **P = 0.01; ***P = 0.001.

increase in the number of released EVs and 2) an enrichment of let-7 family members in the secreted EVs. The connection between estrogen and EVs is a unique finding, as such, we propose a complex mechanism explaining these phenotypes (*SI Appendix,* Fig. S6). The commonality between the two processes relies on the 17β-estradiol-dependent downregulation of miR-149-5p. We postulate that ER regulates miR-149-5p expression by binding its promoter, which harbors an ER-specific binding motif. We confirmed the promoter activity of the ER-binding sequence using luciferase and Chip-qPCR assay. Our hypothesis is supported by independent Chip-Seq datasets, which highlight that ER preferentially interacts with the sequence corresponding to our investigated miR-149-5p promoter region. We indicate that the functional consequences of the downregulation of miR-149-5p, namely the increase in EV production and the modification in miRNA cargo composition, come because of its main regulatory targets, namely *SP1* and *hnRNPA1*. First, we confirmed that the consistent increase in EV production following 17β-estradiol is due to the upregulation of transcription factor SP1, a known target of miR-149-5p, and a confirmed regulator of *nSMase2* in MCF-7 cells (76). Neutral sphingomyelinases (nSMases) have been implicated in EV budding and release from the plasma membrane (47, 77). This evidence further supports our findings, as we have initially shown that the treatment with the specific nSMase inhibitor GW4869 had a noticeable effect on EV production in our cells, counteracting the stimulatory effect induced by 17β-estradiol.

Second, we hypothesized that the modifications in the EV cargo composition, in the form of an ER+ cell–specific upregulation in let-7 miRNAs, come as a result of the regulatory effect of miR-149-5p on the expression of hnRNPA1, as previously described (60). These data are in line with our observation that a reduction of cellular miR-149-5p due to 17β-estradiol treatment corresponded to increased levels of hnRNPA1. Multiple studies are indicating that hnRNPA family members can bind and dictate the loading of an miRNA into EVs, based on the presence of specific motifs in their sequence. The consensus binding site (UAGGGA/U) for hnRNPA1 was found in the let-7 family, as well as described the binding interaction between pri-let-7a and hnRNPA1 in vitro (78). Villarroya-Beltri et al. (18) identified an additional mechanism that implied the sorting of miRNAs into exosomes based on the presence of an hnRNPA2B1-specific consensus motif in their sequence and indicated that a similar mechanism could be valid also for hnRNPA1, given the similarity of its miRNA-binding site. We furtherly indicated this interaction first by highlighting the presence of the hnRNPA1-specific binding motifs in let-7s. Additionally, we demonstrated by RNA–protein pull-down that let-7a-5p and let-7d-5p, two of the most enriched let-7 family members identified in the ER+ cell–derived EVs, directly interact with hnRNPA1. Interestingly, previous studies on EV miRNA signatures did not detect any abundant let-7 family in the exosomes released from MCF-7, MCF-10A, and MDA-MB-231 cells without estrogen stimulation (79). This evidence adds importance to the observed phenotype in ER+ BC cells after treatment with 17β-estradiol.

Our extension of the study by investigating the levels of let-7a-5p and let-7d-5p in the circulating EVs derived from ER+ and TNBC BC patients furtherly indicates the presence of a hormone-dependent mechanism. Pre-menopausal ER+ patients had significantly elevated levels of both let-7 family members in EVs, which might be correlated with the increased average levels of 17β-estradiol in the blood (71). Additionally, the enrichment observed in BC women with elevated BMI might also be correlated with the estrogen-producing properties of the adipose tissue. We are aware that other hormones might additionally contribute to the enrichment of circulating EVs, as was previously pointed out in the case of leptin (10). While the described hormonal mechanisms are not mutually exclusive, their coalescent contribution to the modulation of the EV biogenesis pathway should be considered and investigated [as recently described in ref. (68)].

We also indicate that the ER+-derived EVs after estrogen stimulation might have extensive roles in modulating the TME. The let-7 family is known as tumor-suppressor miRNAs able to inhibit cancer cell proliferation, progression, and metastasis (80). This family has been previously shown to hinder the polarization of tumor-associated macrophages (TAMs) into classical activated immunostimulatory (M1) phenotype by inhibiting IFN-γ (81). In our case, the treatment of M0 macrophages with let-7-enriched EVs derived from 17β-estradiol-stimulated ER+ cells resulted in significant effects on the cytokines involved in macrophage activation, the most relevant being IFN-γ, a key cytokine involved in macrophage M1 activation and polarization. We confirmed this by highlighting the downregulation of IL-12A, one of the IFN-γ's main regulatory targets, both being involved in a costimulatory feedback loop (82). This might be an indicator that, besides the expulsion of tumor-suppressor miRNAs from the BC cells, the secretion of let-7's enriched EVs might also modulate, to some degree, immune signaling in the TME.

We are aware that some results here described could be strengthened in the future. Considering the physiological pre- and post-menopausal variations and heterogeneous dispersion of 17β-estradiol in both cells and TME, we are aware that our described mechanism does not imply a unitary and synchronous response in all ER+ cells following estrogen exposure. Yet, by using a dose range that was in line with the physiological levels of estrogen (100 pM to 1 nM) measured in pre- and post-menopausal women and BC patients, we generated data that confirmed the observations done at higher (and more effective for in vitro studies) dose of estrogens. The setup in the future of a prospective protocol to investigate the levels of let-7 family members in plasma EVs of BC women before and after endocrine therapy could help in elucidating more in deep the role of estrogen in this cancer. Additionally, the complete characterization of the functional effects of the let-7 family–enriched EVs in the TME is an additional topic that requires extensive investigation.

The observations obtained for MCF-10A cells deserve further analyses in the future. These cells, in fact, are ER- but showed an unexpected behavior in the presence of a high dose of 17β-estradiol. These inconsistencies could be explained by the presence in these cells of the alternative receptor for 17β-estradiol GPER that may lead to activation of the downstream pathway after 17β-estradiol binding (36, 83). Although MCF-10A are ER-α negative, the binding of 17β-estradiol to GPER in these cells could activate a certain regulatory effect on the expression of hnRNPA1, as previously described (60). For a more thorough exploration, we also used GPER1-selective agonist and antagonist, but we did not observe any changes in EV release. These observations allow us to exclude the involvement of GPER1 in the EV release mechanism described in this manuscript. Maybe the unexpected slight increase in EV release observed in MCF-10A after 17β-estradiol could be due to residual ER-α.

In conclusion, we discovered a tight link between hormones, miRNAs, and EVs in cell-to-cell communication. Altered hormone secretion acts as a regulator of the EVs released by the cells in a dose-dependent way and contributes to the selection of specific miRNAs to be loaded into EVs. This mechanism could be of particular interest, especially in those diseases that are influenced by hormones such as breast and prostate cancers. Such findings can be further exploited therapeutically to improve the ER+ BC patient's survival.

Materials and Methods

Cells Lines, Media, and Chemical Reagents. MDA-MB-231, MCF-7, BT-474, ZR-75-1, MCF-10A, and THP-1 cell lines were obtained from the American Type Culture Collection (ATCC) (*SI Appendix*, Table S3). Information on culturing conditions is given in *SI Appendix*. Treatment concentrations and reagents are reported in *SI Appendix*.

Cell Transfection with siRNAs and miRNA Inhibitor. Cells (MCF-7, BT-474, MDA-MB-231, ZR-75-1, and MCF-10A) were seeded into 12- or 6-well plates or 15 cm^2 Petri dishes until 80 to 90% confluency was reached. Transfection of cells was performed as described in *SI Appendix*.

EV Purification and Characterization. EVs were obtained from the supernatant of the cells by differential ultracentrifugation described in *SI Appendix*. Due to the small volumes available of BC patient samples, EVs were isolated with ExoQuick (System Biosciences; see *SI Appendix*).

Isolated EV fractions were analyzed and quantified using NanoSight NS500 (NanoSight). Particle concentration and size distribution profiles were obtained using NanoSight Tracking Analysis (NTA) v2.3.0.17 software (NanoSight, more details in *SI Appendix*).

Evaluation of Plasma/Serum EV Content of let-7 Family Members in Breast Cancer Patients. For the test set, human prospective plasma samples were obtained from BC patients after diagnostic biopsy and before therapy (treatment naïve) or surgery as described in ref. (84). The study was approved and supervised by the University of Texas MD Anderson Institutional Review Board (LAB03-0479; LAB90-049; and 2005–0388). For the validation set, 10 mL of serum was prospectively collected just before the time of definitive surgery from stage I-III BC patients. The institutional review board at the University of Texas MD Anderson Cancer Center approved this study (LAB04-0698). Informed consent from all patients was obtained before collecting their blood. Patient characteristics are reported in *SI Appendix*, Table S2. More details are described in *SI Appendix*.

RNA Extraction and qRT-PCR. For the full description of the procedure for RNA extraction and qRT-PCR from cells and EVs, see *SI Appendix*. Probes and primers employed are summarized in *SI Appendix*, Tables S4 and S5.

Microarray Analyses. The full description of miRNA profiling by Affymetrix GeneChip miRNA 3.0 arrays (Affymetrix) is described in *SI Appendix*.

Western Blot. A full description of the methodology is given in *SI Appendix*. The list of antibodies is described in *SI Appendix*, Table S6. Unedited western blot images are reported in Dataset S1.

RNA Pull-Down Assay. Biotinylated let-7a and let-7d probes (Dharmacon) were used for an RNA pull-down assay to prove their direct binding with hnRNPA1 protein. Methodology is described in *SI Appendix*.

Cloning of miR-149-5p Promoter Region and ER1-Binding Site Predictions. The promoters in the region −10 kb upstream and +10 kb downstream of the 5′ ends of the annotated *MIR-149* gene were investigated for the presence of the ER1-binding consensus sequence (agGTCAnngTGACCtg) using UCSC Genome Browser on Human Feb. 2009 (GRCh37/hg19) Assembly. The region containing the ER1-binding motif located −5,500 bp from the miR-149 sequence was cloned into pCR™ 2.1-TOPO® TA vector using the TOPO TA cloning kit (Cat No K4500-01, Invitrogen) and DH5α competent cells. The "5500" region was mutated using the Quick Change II XL Site-Directed Mutagenesis kit (Agilent Technologies) following manufacturer's instructions. Mutagenic primers were designed at www.agilent.com/genomics/qcpd. The methodology is described in *SI Appendix*.

Chip-Seq Database Analysis. Chip-Seq next-generation sequencing data were downloaded from a publicly available Chip-Seq dataset (45) and analyzed using the CLC Genomic Workbench v22. The methodology is in *SI Appendix*.

Chip-qPCR. MCF-7 and MDA-MB-231 cells were seeded at a density of 2×10^6 cells per 12-cm Petri dish in DMEM/F12 medium (Corning) supplemented with 10% FBS (Sigma-Aldrich), cultured, and stimulated in the same conditions as described in *SI Appendix*. Primer sequences are provided in *SI Appendix*, Table S5.

Luciferase Reporter Assay. PCR products were cloned into pGL3-TK promoter vector following *BamHI* restriction enzyme digestion and inserted downstream of the Firefly luciferase gene, driven by the TK promoter, as described in ref. (44). More details are given in *SI Appendix*.

Treatment of THP-1 Cells with MCF-7-Derived EVs. THP-1 cells seeding and treatment are described in *SI Appendix*.

In Silico and Statistical Analyses. All statistical and in silico analyses are described in *SI Appendix*.

Data, Materials, and Software Availability. The microarray data presented in this study (CEL files and normalized miRNA expression table) have been deposited in NCBI's Gene Expression Omnibus (GEO) and are accessible through GEO Series accession number GSE127787 (85).

ACKNOWLEDGMENTS. G.A.C. is the Felix L. Haas-Endowed Professor in Basic Science. Work in Dr. Calin's laboratory is supported by the NCI grants 1R01 CA182905-01 and 1R01CA222007-01A1, an NIGMS 1R01GM122775-01 grant, a DoD Idea Award W81XWH-21-1-0030, a Team DOD grant in Gastric Cancer W81XWH-21-1-0715, a Chronic Lymphocytic Leukemia Moonshot Flagship project, a CLL Global Research Foundation 2019 grant, a CLL Global Research Foundation 2020 grant, a CLL Global Research Foundation 2022 grant, The G. Harold & Leila Y. Mathers Foundation, two grants from Torrey Coast Foundation, an Institutional Research Grant, and a Development Grant associated with the Brain SPORE 2P50CA127001. R.D. and A.J. were supported by the European Union's Horizon 2020 research and innovation program under the Marie Skłodowska-Curie grant agreement no. 824036. B.P. was supported by a Fulbright Research Scholarships (year 2018). EK is supported by Helse Nord (HNF1585-21). M.F. is supported by the NIH/NCI grants R01CA215753-01A1 and R01CA219024-01A1. M.P.D. is a participant in the BIH-Charité Junior Clinical Scientist Program funded by the Charité – Universitätsmedizin Berlin and the Berlin Institute of Health and is supported by a DKTK Berlin Young Investigator Grant 2022 and by the Berliner Krebsgesellschaft (DRFF202204). A.M.T. was supported by the CPRIT Research Training Program (RP170067). Figures depicting the experimental design and mechanism were created using BioRender.com.

Author affiliations: [a]Department of Translational Molecular Pathology, The University of Texas MD Anderson Cancer Center, Houston, TX 77030; [b]The Research Center for Functional Genomics, Biomedicine and Translational Medicine, Iuliu Hatieganu University of Medicine and Pharmacy, 400337 Cluj Napoca, Romania; [c]Italian Institute for Genomic Medicine, c/o FPO-IRCCS Candiolo, 10060 Candiolo, Italy; [d]Candiolo Cancer Institute, FPO-IRCCS, 10060 Candiolo, Italy; [e]Department of Experimental Therapeutics, The University of Texas MD Anderson Cancer Center, Houston, TX 77030; [f]Department of Medical Oncology, The First Affiliated Hospital of Xi'an Jiaotong University, Xi'an, 710061 Shaanxi, China; [g]Department of Oncology-Pathology, Karolinska Institutet, Karolinska University Hospital, 17164 Solna, Sweden; [h]Medical Biochemistry Department, Medical Research and Clinical Studies Institute, National Research Centre, Cairo 12622, Egypt; [i]Department of Medical Biology, Faculty of Health Sciences, UiT, The Artic University of Norway, N-9037 Tromso, Norway; [j]Centre for Clinical Research and Education, University Hospital of North Norway, N-9037 Tromso, Norway; [k]Institute of Pathology, Charité-Universitätsmedizin Berlin, Corporate Member of Freie Universität Berlin, Humboldt-Universität zu Berlin, 10178 Berlin, Germany; [l]German Cancer Research Center (DKFZ), Partner Site Berlin, and German Cancer Consortium (DKTK), 69120 Heidelberg, Germany; [m]Berlin Institute of Health, 10178 Berlin, Germany; [n]Department of Breast Surgery, Zhejiang Cancer Hospital, Hangzhou, 310022 Zhejiang, P.R. China; [o]University of Hawaii Cancer Center, Cancer Biology Program, Honolulu, HI 96813; [p]Department of Research Imaging, Dana Farber Cancer Institute, Boston, MA 02215; [q]College of Natural Sciences, The University of Texas at Austin, Austin, TX 78712; [r]Department of Chemistry, Mount Holyoke College, South Hadley, MA 01075; [s]Department of Pediatrics, Duke University, Durham, NC 27708; [t]Department of Nephrology and Medical Intensive Care, Charité—Universitätsmedizin Berlin, 10117 Berlin, Germany; [u]Department of Breast Medical Oncology, Division of Cancer Medicine, The University of Texas MD Anderson Cancer Center, Houston, TX 77030; [v]Center for RNA Interference and Non-Coding RNAs, The University of Texas MD Anderson Cancer Center, Houston, TX 77030; [w]Breast Surgical Oncology, Division of Cancer Medicine, The University of Texas MD Anderson Cancer Center, Houston, TX 77030; [x]Department of Biochemistry and Molecular Biology, Stanley S Scott Cancer Center, Louisiana State University School of Medicine, New Orleans, LA 70112; and [y]Center for Cancer and Immunology Research, Children's National Hospital, Washington DC 20010

Author contributions: R.D., B.P., S.A., and G.A.C. designed research; R.D., B.P., X.F., M.C.D.I.S., A.J., L.P., S.M.E-D., L.F., M.P.D., R.B., Y.L., L.B., J.D., M.S., A.M.T., M.B., A.M.G., I.B.-N., A.L., B.A., and S.A. performed research; M.C.D.I.S., L.F., E.K., M.C., F.D.V., C.S.H., and S.K.A. contributed new reagents/analytic tools; R.D., B.P., X.F., M.C.D.I.S., M.C., A.J., L.P., E.K., M.P.D., R.B., D.F., M.S., C.P., A.M.G., C.I., S.M., I.B-N., and M.F. analyzed data; R.D. and B.P. interpretation of the data; X.F., M.C.D.I.S., and G.A.C. revised the paper interpretation of the data; A.J., L.P., S.M.E.-D., and L.F. revised the paper; E.K., M.P.D., R.B., F.D.V., M.B., and M.F. revision of the paper and gave interpretation of the data; Y.L., M.C., L.B., J.D., D.F., M.S., A.M.T., C.P., A.M.G., C.I., and I.B.-N. revision of the paper; S.M.E.-D. revised the paper; C.S.H., S.K.A., A.L., and B.A. revised the paper for the human study contribution; S.A. revision of the paper and interpretation of data; and R.D., B.P., and G.A.C. wrote the paper.

1. K. O'Brien, K. Breyne, S. Ughetto, L. C. Laurent, X. O. Breakefield, RNA delivery by extracellular vesicles in mammalian cells and its applications. *Nat. Rev. Mol. Cell Biol.* **21**, 585–606 (2020).
2. M. Mathieu, L. Martin-Jaular, G. Lavieu, C. Thery, Specificities of secretion and uptake of exosomes and other extracellular vesicles for cell-to-cell communication. *Nat. Cell Biol.* **21**, 9–17 (2019).
3. H. Valadi *et al.*, Exosome-mediated transfer of mRNAs and microRNAs is a novel mechanism of genetic exchange between cells. *Nat. Cell Biol.* **9**, 654–659 (2007).
4. C. Tetta, E. Ghigo, L. Silengo, M. C. Deregibus, G. Camussi, Extracellular vesicles as an emerging mechanism of cell-to-cell communication. *Endocrine* **44**, 11–19 (2013).
5. D. K. Jeppesen, Q. Zhang, J. L. Franklin, R. J. Coffey, Extracellular vesicles and nanoparticles: Emerging complexities. *Trends Cell Biol.* (2023), 10.1016/j.tcb.2023.01.002.
6. L. H. Lv *et al.*, Anticancer drugs cause release of exosomes with heat shock proteins from human hepatocellular carcinoma cells that elicit effective natural killer cell antitumor responses in vitro. *J. Biol. Chem.* **287**, 15874–15885 (2012).
7. O. G. de Jong *et al.*, Cellular stress conditions are reflected in the protein and RNA content of endothelial cell-derived exosomes. *J. Extracell. Vesicles* **1** (2012).
8. R. Kalluri, V. S. LeBleu, The biology, function, and biomedical applications of exosomes. *Science* **367** (2020).
9. C. Villarroya-Beltri, F. Baixauli, C. Gutierrez-Vazquez, F. Sanchez-Madrid, M. Mittelbrunn, Sorting it out: Regulation of exosome loading. *Semin. Cancer Biol.* **28**, 3–13 (2014).
10. C. Giordano *et al.*, Leptin modulates exosome biogenesis in breast cancer cells: An additional mechanism in cell-to-cell communication. *J. Cli.n Med.* **8** (2019).
11. S. Anfossi, A. Babayan, K. Pantel, G. A. Calin, Clinical utility of circulating non-coding RNAs - an update. *Nat. Rev. Clin. Oncol.* **15**, 541–563 (2018).
12. R. Bayraktar, K. Van Roosbroeck, G. A. Calin, Cell-to-cell communication: microRNAs as hormones. *Mol. Oncol.* **11**, 1673–1686 (2017).
13. M. Fabbri, MicroRNAs and miRceptors: A new mechanism of action for intercellular communication. *Philos. Trans. R. Soc. Lond. B Biol. Sci.* **373** (2018).
14. B. Pardini, G. A. Calin, MicroRNAs and Long Non-Coding RNAs and Their Hormone-Like Activities in Cancer. *Cancers* **11** (2019).
15. B. H. Sung, T. Ketova, D. Hoshino, A. Zijlstra, A. M. Weaver, Directional cell movement through tissues is controlled by exosome secretion. *Nat. Commun.* **6**, 7164 (2015).
16. M. Mittelbrunn *et al.*, Unidirectional transfer of microRNA-loaded exosomes from T cells to antigen-presenting cells. *Nat. Comm.* **2**, 282 (2011).
17. T. Fiskaa *et al.*, Distinct small RNA signatures in extracellular vesicles derived from breast cancer cell lines. *PLoS One* **11**, e0161824. (2016).
18. C. Villarroya-Beltri *et al.*, Sumoylated hnRNPA2B1 controls the sorting of miRNAs into exosomes through binding to specific motifs. *Nat. Commun.* **4**, 2980 (2013).
19. R. L. Siegel, K. D. Miller, H. E. Fuchs, A. Jemal, Cancer statistics. *CA: Cancer. J. Clin.* **72**, 7–33 (2022).
20. A. N. Giaquinto *et al.*, Breast cancer statistics. *CA: Cancer J. Clin.* **72**, 524–541 (2022).
21. Y. Li *et al.*, Clinicopathological characteristics and breast cancer-specific survival of patients with single hormone receptor-positive breast cancer. *JAMA Netw. Open* **3**, e1918160. (2020).
22. X. H. Zhang, M. Giuliano, M. V. Trivedi, R. Schiff, C. K. Osborne, Metastasis dormancy in estrogen receptor-positive breast cancer. *Clin. Cancer Res.* **19**, 6389–6397 (2013).
23. F. Bertucci, P. Finetti, A. Goncalves, D. Birnbaum, The therapeutic response of ER+/HER2- breast cancers differs according to the molecular Basal or Luminal subtype *NPJ Breast Cancer* **6**, 8 (2020).
24. F. Cardoso *et al.*, Early breast cancer: ESMO Clinical Practice Guidelines for diagnosis, treatment and follow-up. *Ann. Oncol.* **30**, 1674 (2019).
25. F. Bertucci *et al.*, Genomic characterization of metastatic breast cancers. *Nature* **569**, 560–564 (2019).
26. G. Maillot *et al.*, Widespread estrogen-dependent repression of micrornas involved in breast tumor cell growth. *Cancer Res.* **69**, 8332–8340 (2009).
27. G. Di Leva *et al.*, Estrogen mediated-activation of miR-191/425 cluster modulates tumorigenicity of breast cancer cells depending on estrogen receptor status. *PLoS Genet.* **9**, e1003311. (2013).
28. I. K. Guttilla, B. D. Adams, B. A. White, ERalpha, microRNAs, and the epithelial-mesenchymal transition in breast cancer. *Trends Endocrinol. Metab.* **23**, 73–82 (2012).
29. M. J. G. Milevskiy *et al.*, MicroRNA-196a is regulated by ER and is a prognostic biomarker in ER+ breast cancer. *Br. J. Cancer* **120**, 621–632 (2019).
30. E. W. Howard, X. Yang, microRNA regulation in estrogen receptor-positive breast cancer and endocrine therapy. *Biol. Proced. Online* **20**, 17 (2018).
31. P. Bhat-Nakshatri *et al.*, Estradiol-regulated microRNAs control estradiol response in breast cancer cells. *Nucleic Acids Res.* **37**, 4850–4861 (2009).
32. C. J. Gruber, W. Tschugguel, C. Schneeberger, J. C. Huber, Production and actions of estrogens. *N. Engl. J. Med.* **346**, 340–352 (2002).
33. H. T. Depypere *et al.*, The serum estradiol concentration is the main determinant of the estradiol concentration in normal breast tissue. *Maturitas* **81**, 42–45 (2015).
34. M. G. Ghosh, D. A. Thompson, R. J. Weigel, PDZK1 and GREB1 are estrogen-regulated genes expressed in hormone-responsive breast cancer. *Cancer Res.* **60**, 6367–6375 (2000).
35. Y. W. Leu *et al.*, Loss of estrogen receptor signaling triggers epigenetic silencing of downstream targets in breast cancer. *Cancer Res.* **64**, 8184–8192 (2004).
36. E. J. Filardo, P. Thomas, Minireview: G protein-coupled estrogen receptor-1, GPER-1: Its mechanism of action and role in female reproductive cancer, renal and vascular physiology. *Endocrinology* **153**, 2953–2962 (2012).
37. H. T. Magruder *et al.*, The G protein-coupled estrogen receptor-1, GPER-1, promotes fibrillogenesis via a Shc-dependent pathway resulting in anchorage-independent growth. *Horm. Cancer* **5**, 390–404 (2014).
38. C. G. Bologa *et al.*, Virtual and biomolecular screening converge on a selective agonist for GPR30. *Nat. Chem. Biol.* **2**, 207–212 (2006).
39. M. K. Dennis *et al.*, Identification of a GPER/GPR30 antagonist with improved estrogen receptor counterselectivity. *J. Steroid Biochem. Mol. Biol.* **127**, 358–366 (2011).
40. L. C. Hodges *et al.*, Tamoxifen functions as a molecular agonist inducing cell cycle-associated genes in breast cancer cells. *Mol. Cancer Res.* **1**, 300–311 (2003).
41. J. Frasor *et al.*, Gene expression preferentially regulated by tamoxifen in breast cancer cells and correlations with clinical outcome. *Cancer Res.* **66**, 7334–7340 (2006).
42. C. Y. Lin *et al.*, Discovery of estrogen receptor alpha target genes and response elements in breast tumor cells. *Genome Biol.* **5**, R66 (2004).
43. B. Chen, Y. Wang, S. E. Kane, S. Chen, Improvement of sensitivity to tamoxifen in estrogen receptor-positive and Herceptin-resistant breast cancer cells. *J. Mol. Endocrinol.* **41**, 367–377 (2008).
44. A. Nardone *et al.*, The oral selective oestrogen receptor degrader (SERD) AZD9496 is comparable to fulvestrant in antagonising ER and circumventing endocrine resistance. *Br. J. Cancer* **120**, 331–339 (2019).
45. I. Paterni, C. Granchi, J. A. Katzenellenbogen, F. Minutolo, Estrogen receptors alpha (ERalpha) and beta (ERbeta): Subtype-selective ligands and clinical potential. *Steroids* **90**, 13–29 (2014).
46. C. Luberto *et al.*, Inhibition of tumor necrosis factor-induced cell death in MCF7 by a novel inhibitor of neutral sphingomyelinase. *J. Biol. Chem.* **277**, 41128–41139 (2002).
47. K. Trajkovic *et al.*, Ceramide triggers budding of exosome vesicles into multivesicular endosomes. *Science* **319**, 1244–1247 (2008).
48. E. N. Nolte-'t Hoen *et al.*, Deep sequencing of RNA from immune cell-derived vesicles uncovers the selective incorporation of small non-coding RNA biotypes with potential regulatory functions. *Nucleic Acids Res.* **40**, 9272–9285 (2012).
49. J. Sun *et al.*, RAC1 plays an essential role in estrogen receptor alpha function in breast cancer cells. *Oncogene* **40**, 5950–5962 (2021).
50. J. Ghose, N. P. Bhattacharyya, Transcriptional regulation of microRNA-100, -146a, and -150 genes by p53 and NFkappaB p65/RelA in mouse striatal STHdh(Q7)/ Hdh(Q7) cells and human cervical carcinoma HeLa cells. *RNA Biol.* **12**, 457–477 (2015).
51. T. C. Chang, M. Pertea, S. Lee, S. L. Salzberg, J. T. Mendell, Genome-wide annotation of microRNA primary transcript structures reveals novel regulatory mechanisms. *Genome Res.* **25**, 1401–1409 (2015).
52. Q. Liu *et al.*, Identification of active miRNA promoters from nuclear run-on RNA sequencing. *Nucleic Acids Res.* **45**, e121. (2017).
53. J. D. Stender *et al.*, Genome-wide analysis of estrogen receptor alpha DNA binding and tethering mechanisms identifies Runx1 as a novel tethering factor in receptor-mediated transcriptional activation. *Mol. Cell. Biol.* **30**, 3943–3955 (2010).
54. U. A. Orom *et al.*, Long noncoding RNAs with enhancer-like function in human cells. *Cell* **143**, 46–58 (2010).
55. A. E. Rosenblatt *et al.*, Inhibition of the Rho GTPase, Rac1, decreases estrogen receptor levels and is a novel therapeutic strategy in breast cancer. *Endocr.-Relat. Cancer* **18**, 207–219 (2011).
56. M. Garcia-Arencibia, N. Davila, J. Campion, M. Carmen Carranza, C. Calle, Identification of two functional estrogen response elements complexed with AP-1-like sites in the human insulin receptor gene promoter. *J. Steroid Biochem. Mol. Biol.* **94**, 1–14 (2005).
57. F. Wang *et al.*, SP1 mediates the link between methylation of the tumour suppressor miR-149 and outcome in colorectal cancer. *J. Pathol.* **229**, 12–24 (2013).
58. Y. Teng *et al.*, MVP-mediated exosomal sorting of miR-193a promotes colon cancer progression. *Nat. Commun.* **8**, 14448 (2017).
59. L. Santangelo *et al.*, The RNA-Binding Protein SYNCRIP Is a Component of the Hepatocyte Exosomal Machinery Controlling MicroRNA Sorting. *Cell Rep.* **17**, 799–808 (2016).
60. E. Sokol *et al.*, microRNA-mediated regulation of splicing factors SRSF1, SRSF2 and hnRNP A1 in context of their alternatively spliced 3'UTRs. *Exp. Cell Res.* **363**, 208–217 (2018).
61. W. C. Park *et al.*, Comparative expression patterns and diagnostic efficacies of SR splicing factors and HNRNPA1 in gastric and colorectal cancer. *BMC Cancer* **16**, 358 (2016).
62. R. Roy *et al.*, hnRNPA1 couples nuclear export and translation of specific mRNAs downstream of FGF-2/S6K2 signalling. *Nucleic Acids Res.* **42**, 12483–12497 (2014).
63. S. Li *et al.*, Identification of an aptamer targeting hnRNP A1 by tissue slide-based SELEX. *J. Pathol.* **218**, 327–336 (2009).
64. X. Yu, M. Odenthal, J. W. Fries, Exosomes as miRNA Carriers: Formation-Function-Future. *Int. J. Mol. Sci.* **17** (2016).
65. R. Garcia-Martin *et al.*, MicroRNA sequence codes for small extracellular vesicle release and cellular retention. *Nature* **601**, 446–451 (2022).
66. T. Janas, M. M. Janas, K. Sapon, Mechanisms of RNA loading into exosomes. *FEBS Lett.* **589**, 1391–1398 (2015).
67. T. Li *et al.*, Sumoylation of heterogeneous nuclear ribonucleoproteins, zinc finger proteins, and nuclear pore complex proteins: A proteomic analysis. *P. Natl. Acad. Sci. U.S.A.* **101**, 8551–8556 (2004).
68. S. Karvinen *et al.*, Extracellular vesicles and high-density lipoproteins: Exercise and oestrogen-responsive small RNA carriers. *J. Extracell. Vesicles* **12**, e12308. (2023).
69. R. V. Considine *et al.*, Serum immunoreactive-leptin concentrations in normal-weight and obese humans. *N. Engl. J. Med.* **334**, 292–295 (1996).
70. C. Baer *et al.*, Suppression of microRNA activity amplifies IFN-gamma-induced macrophage activation and promotes anti-tumour immunity. *Nat. Cell Biol.* **18**, 790–802 (2016).
71. Z. Wang *et al.*, miRNA let-7b modulates macrophage polarization and enhances tumor-associated macrophages to promote angiogenesis and mobility in prostate cancer. *Sci. Rep.* **6**, 25602 (2016).
72. S. Jiang, W. Yan, S. E. Wang, D. Baltimore, Dual mechanisms of posttranscriptional regulation of Tet2 by Let-7 microRNA in macrophages. *Proc. Natl. Acad. Sci. U.S.A.* **116**, 12416–12421 (2019).
73. Y. P. Xu *et al.*, Tumor suppressor TET2 promotes cancer immunity and immunotherapy efficacy. *J. Clin. Investig.* **129**, 4316–4331 (2019).
74. T. Hamza, J. B. Barnett, B. Li, Interleukin 12 a key immunoregulatory cytokine in infection applications. *Int. J. Mol. Sci.* **11**, 789–806 (2010).
75. L. B. Ivashkiv, IFNgamma: signalling, epigenetics and roles in immunity, metabolism, disease and cancer immunotherapy. *Nat. Rev. Immunol.* **18**, 545–558 (2018).
76. H. Ito *et al.*, Transcriptional regulation of neutral sphingomyelinase 2 in all-trans retinoic acid-treated human breast cancer cell line, MCF-7. *J. Biochem.* **151**, 599–610 (2012).
77. K. Menck *et al.*, Neutral sphingomyelinases control extracellular vesicles budding from the plasma membrane. *J. Extracell. Vesicles* **6**, 1378056 (2017).
78. G. Michlewski, J. F. Caceres, Antagonistic role of hnRNP A1 and KSRP in the regulation of let-7a biogenesis. *Nat. Struct. Mol. Biol.* **17**, 1011–1018 (2010).
79. B. N. Hannafon *et al.*, Plasma exosome microRNAs are indicative of breast cancer. *Breast Cancer Res.* **18**, 90 (2016).
80. X. Sun, J. Liu, C. Xu, S. C. Tang, H. Ren, The insights of Let-7 miRNAs in oncogenesis and stem cell potency. *J. Cell. Mol. Med.* **20**, 1779–1788 (2016).
81. S. Mohapatra, C. Pioppini, B. Ozpolat, G. A. Calin, Non-coding RNAs regulation of macrophage polarization in cancer. *Mol. Cancer* **20**, 24 (2021).
82. U. Grohmann *et al.*, Positive regulatory role of IL-12 in macrophages and modulation by IFN-gamma. *J. Immunol.* **167**, 221–227 (2001).
83. A. L. Scaling, E. R. Prossnitz, H. J. Hathaway, GPER mediates estrogen-induced signaling and proliferation in human breast epithelial cells and normal and malignant breast. *Horm. Cancer* **5**, 146–160 (2014).
84. J. F. Fahrmann *et al.*, Association between plasma diacetylspermine and tumor spermine synthase with outcome in triple-negative breast cancer. *J. Natl. Cancer Inst.* **112**, 607–616 (2020).
85. B. Pardini, G. Calin, 17β-estradiol regulates the release of exosomes via miR-149-5p and hnRNPA2/B1 in ER+ breast cancer cells. Gene Expression Omnibus. https://www.ncbi.nlm.nih.gov/geo/query/acc.cgi?acc=GSE127787. Deposited 4 March 2019.